Electroosmotic Flow Enhancement in Carbon Nanotube Membranes

Davide Mattia,[1*] Hannah Leese,[1] Francesco Calabrò[2]

1 Department of Chemical Engineering, University of Bath, Bath, BA27AY, UK
2 DIEI, Università di Cassino, Cassino, I-03043, Italy,

Keywords: electroosmotic flow, carbon nanotubes, membranes, electroosmosis

Summary

In this work, experimental evidence of the presence of electroosmotic flow (EOF) in carbon nanotube membranes with diameters close to or in the region of electrical double layer overlap is presented for two different electrolytes for the first time. No electroosmotic flow in this region should be present according to the simplified theoretical framework commonly used for EOF in micrometre size channels. The simplifying assumptions concern primarily the electrolyte charge density structure, based on the Poisson-Boltzmann (P-B) equation. Here a numerical analysis of the solutions for the simplified case and for the non-linear and the linearized P-B equations, is compared to experimental data. Results show that the simplified solution produces a significant deviation from experimental data, whereas the linearized solution of the P-B equation can be adopted with little error compared to the full P-B case.
This work opens the way to using electroosmotic pumping in a wide range of applications, from membrane-based ultrafiltration and nanofiltration (as a more efficient alternative to mechanical pumping at the nanoscale) to further miniaturization of lab-on-a-chip devices at the nanoscale for *in vivo* implantation.

Introduction

Electroosmotic flow, the movement of an electrolyte relative to a charged surface due to an external electric field, is commonly used as a no-moving parts pumping system in diverse applications, from high-speed chromatography to soil remediation to lab-on-a-chip and portable analytical and medical devices applications (1). When an electrolyte is in contact with a dielectric (charged surface), an electrical double layer (EDL) is generated, with a dynamic imbalance of charge between the EDL and the bulk of the electrolyte. When an external electric field is applied tangentially to the axis of a channel with a charged surface, the ions in the EDL are attracted to the electrodes of opposite polarity generating flow in the EDL and pulling the rest of the electro-neutral bulk fluid with it. The result is a net flow with the flow velocity being zero at the wall (no-slip condition) increasing to the maximum within the EDL and then remaining quasi-constant in the electro-neutral bulk. The result is a flat velocity profile similar to plug flow (2). The thickness of the EDL is called the Debye length and, typically, varies between 1-100 nanometres (1). As such, an appreciable amount of

*Author for correspondence (d.mattia@bath.ac.uk)
†Present address: Department of Chemical Engineering, University of Bath, Bath, BA27AY, UK

electroosmotic flow can be generated only in channels one or two orders of magnitude larger that the Debye length, hence its wide use to lab-on-a-chip and microfluidics-type applications but not larger scale pumping applications (1). On the other hand, the commonly used theoretical framework for EOF assumes that as the channel size approaches the Debye length, an overlap between the EDLs occurs, so that a dynamic accumulation of one ion species near the wall becomes impossible, since all the channel would now be charged (2). As a result, the electro-osmotic flow would be strongly suppressed (3). In recent years, though, some evidence has appeared that contradicts this conclusion. EOF was observed in a functionalized carbon nanotube (CNT) membrane with diameters ranging from 1.5 to 7 nm (4). Although not mentioned by the authors, it is likely that the EDLs were overlapped as the concentrations of the buffer used would produce Debye lengths of ~ 5-10 nm. Also, measurements in track-etched polymer membranes with pores of approximately 15 nm showed the persistence of EOF close to, but not in, the electric double layer overlap region (5). More recently, the present authors have demonstrated the presence of EOF in anodic alumina membranes in the overlap region (6). Simulations of electrokinetic phenomena also appear to contradict the theoretical predictions of EOF suppression: Simulations of EOF in 6.5 nm diameter channels showed higher than expected electroosmotic mobility of ions near the channel wall and a flat velocity profile in the Stern layer (though an 'approximately parabolic' profile was observed in the middle of the channel) (7). A flat velocity profile was also observed for simulations of EOF in nanotubes (8), due to nanoscale confinement effects on the electrolyte charge distribution inside the nanotubes (9).

In this work, the presence of net electroosmotic flow of two electrolytic solutions through carbon nanotube membranes (CNMs) near to or in the region of electrical double layer overlap is demonstrated experimentally. A complete mathematical analysis of the equations of flow and charge distributions demonstrates the limits of the simplified theory commonly used to explain EOF at the micrometre scale and the need to use the more complex, full model to capture non-linear effects observed at the nanoscale.

Governing Laws

The Navier-Stokes equation describing the steady-state flow of an incompressible symmetric electrolyte in a cylindrical capillary of length L and radius R subject to an external pressure gradient ($\Delta p / L$) and an external homogenous electrostatic field, both acting only in the axial direction, is (2):

$$\frac{1}{r}\frac{\partial}{\partial r}\left(r\frac{\partial u}{\partial r}\right)+\frac{\Delta p}{\eta L}+\rho_{el}\frac{\Delta\phi}{\eta L}=0 \qquad [1]$$

where η is the electrolyte's viscosity, ρ_{el} is the electrolyte charge density, $\Delta\phi$ is the applied electrostatic potential, which results in an electric field $E=\Delta\phi/L$. The electrolyte charge density is linked to the electrostatic potential in the capillary via the Poisson relation: $\nabla^2\phi=-\rho_{el}/\varepsilon$, where ε is the relative permittivity.

Double integration with the no-slip boundary condition, $u\left(r=R\right)=0$ and $\partial_r u\left(r=0\right)=0$ yields the velocity profile in a single channel (3):

$$u(r) = \frac{R^2}{4\eta}\frac{\Delta p}{L}\left(1-\frac{r^2}{R^2}\right)+\frac{\varepsilon\zeta}{\eta}\left(1-\frac{\phi}{\zeta}\right) \quad [2]$$

where $\zeta = \phi(r = R)$, the so-called zeta potential.

In passing from a single capillary to a membrane, assumptions regarding the membrane pore structure have to be made. For a membrane consisting of a bundle of cylindrical capillaries the membrane porosity ψ is:

$$\psi = \sum_{i=1}^{n}\frac{\pi R_i^2}{A_m} \approx \frac{n\pi R^2}{A_m} \quad [3]$$

where A_m is the membrane cross-sectional area. The second relation is valid only when the membrane has a narrow pore size distribution, as is the case in the present work(6, 10).

Integration of Eq. [2], over the area of a membrane of porosity ψ and tortuosity τ, yields the total flow rate:

$$Q_T = Q_{\Delta P} + Q_{EO} = \frac{\psi A}{\tau}\left[\frac{\varepsilon\zeta}{\eta}\frac{\Delta V_{eff}}{L}F+\frac{R^2\Delta p}{8\eta L}\right] \quad [4]$$

where the potential field over the thickness of the membrane has been replaced with the effective voltage potential, $E = \Delta V_{eff} / L$, and F is the integral of the electrostatic potential across the channel cross-section (11):

$$F := \int_0^R\left(1-\frac{\phi}{\zeta}\right)\frac{2r}{R^2}dr \quad [5]$$

To obtain an explicit solution for the flow rate, an expression for the function ϕ must be derived via the Poisson-Boltzmann equation, which, for a symmetric (z=1) electrolyte of ionic strength c_0 is (2):

$$\frac{1}{r}\frac{\partial}{\partial r}\left(r\frac{\partial}{\partial r}\phi\right) = -\frac{\rho_{el}(r)}{\varepsilon} = \frac{2eN_A c_0}{\varepsilon}\sinh\left(\frac{e\phi}{k_B T}\right) \quad [6]$$

where k_B, and T are the Boltzmann constant and temperature, respectively; N_A and e are Avogardo's number and the electronic charge, respectively; $\varepsilon = \varepsilon_r\varepsilon_0$ where ε_r and ε_0 are the relative permittivity of the electrolyte and the vacuum permittivity, respectively. The above equation can only be solved numerically (12).

When $\frac{e\zeta}{k_B T} \ll 1$, known as the Debye-Hückel approximation, the P-B is linearized as:

$$\frac{1}{r}\frac{\partial}{\partial r}\left(r\frac{\partial}{\partial r}\phi\right)=\frac{\phi}{\lambda_D^2} \qquad [7]$$

where $\lambda_D=\sqrt{\frac{\varepsilon k_B T}{2N_A e^2 c_0}}$ is the Debye length for a monovalent binary electrolyte (2).

The analytical solution to Eq. [7] is:

$$\phi(r)=\zeta\frac{I_0\left(\frac{r}{\lambda_D}\right)}{I_0\left(\frac{R}{\lambda_D}\right)} \qquad [8]$$

where I_0 is the zero-order modified Bessel function of the first kind (2). For a symmetric electrolyte ($z=1$) and at 20 °C, the Debye-Hückel approximation is considered to be valid when $|\zeta| \ll 25$ mV (1). For most materials traditionally used to create electroosmotic pumps like glass, silica, or alumina, the zeta potential is much higher, of the order of 100 mV (11). In this case, it has been shown the solution to the linearized Eq. [7] rather than the more complex numerical solution of Eq. [6] can be used only when $R/\lambda_D > 10$ (13). For lower values of this ratio, significant deviations from the exact solution are observed. The zeta potential of the carbon nanotubes used here is -17.3 mV (14), which suggests that the Debye-Hückel approximation could be profitably used. This will be confirmed in the next section by comparing the linearized solution in Eq. [8] to the solution to the full P-B equation calculated numerically. When $R/\lambda_D \sim 100$, the value of the function F in Eq.[4] is close to unity. The conditions above have all been derived experimentally. They can also be generalized theoretically by considering a Taylor expansion of the electroosmotic flow (EOF) velocity profile only (the pressure-driven term has been omitted for clarity) resulting from using Eq.[8] (2):

$$u_{EOF}(r)\approx\frac{R^2}{4\lambda_D^2}\left[1-\frac{r^2}{R^2}\right]\frac{\varepsilon\zeta}{\eta}\frac{\Delta V_{eff}}{L}+\mathcal{O}\left(\left(\frac{R}{\lambda_D}\right)^2\right) \qquad [9]$$

If one now considers the ratio of the maximal EOF velocity $u(r=0)$ against the electroosmotic velocity $u_{EO}=\frac{\varepsilon\zeta}{\eta}\frac{\Delta V_{eff}}{L}$, then (2):

$$\begin{aligned} &u_{EOF}(r=0)/u_{EO}\approx 1 \text{ for } R/\lambda_D \gg 1 \\ &u_{EOF}(r=0)/u_{EO}\approx R^2/4\lambda_D^2 \text{ for } R/\lambda_D \le 1 \end{aligned} \qquad [10]$$

The first condition above mean that when the channel radius is much larger than the Debye length, the EOF velocity is equal to the electroosmotic one across the whole channel, yielding a flat velocity profile similar to

plug flow, as discussed earlier (Fig. S1). Therefore $F \sim 1$, yielding the following simplified expression for the total flow rate in Eq.[4], commonly used in all EO applications at the micrometre scale:

$$Q = Q_{\Delta P} + Q_{EO} = \frac{\psi A}{\tau}\left[\frac{\varepsilon\zeta}{\eta}\frac{\Delta V_{eff}}{L} + \frac{R^2\Delta p}{8\eta L}\right] \quad [11]$$

On the other hand, the second condition in Eq.[10] shows that when the channel radius is equal to or smaller than the Debye length, the maximal EOF velocity decreases very rapidly to zero (Fig. S1) and the EOF is suppressed (2). As such Eq.[11] cannot be used when the channel size is close to the Debye length (in the region of EDL overlap) as it leads to significant deviations from Eq.[4] (13).

Materials and Methods

CNT Membrane Fabrication

The CNMs were produced via non-catalytic chemical vapour deposition (CVD) in anodic alumina membrane (AAMs) templates. The AAMs were produced via the electrochemical anodization of aluminium, described in detail in (10). The advantage of using AAMs as templates is that their pore size and thickness can be accurately controlled via the anodization parameters.

Once formed, the AAMs were slowly (1 °C/min) annealed to 900 °C. This is a critical step as alumina undergoes several phase transitions in this temperature range with significant changes in the thermal expansion coefficient. Absence of annealing will induce warping and, eventually, disintegration of the AAM during the CVD process to fabricate the CNT membranes (15).

The CVD process to form the CNT membrane has been described in detail elsewhere (16). Briefly, the AAMs were placed in a quartz tube reactor and heated up to 670 °C at 10 °C/min under 50 sccm of argon. Once the set temperature was reached, the flow was switched to a mixture of ethylene and argon (30:70 volume ratio) for a total flow of 20 to 120 sccm and kept for 2-10 hours. At the chosen reaction temperature, ethylene decomposes and a conformal coating of carbon is deposited on the outer and inner surfaces of the template, resulting in the formation of a carbon nanotube membrane. At the end of the reaction period, the CNT membranes were allowed to cool under argon flow until room temperature was reached.

The CNT membranes were characterized using scanning electron microscopy (FEI Supra 50 and JEOL FESEM) to evaluate porosity (due to the regular cross-section and absence of internal branching (10), surface porosity is representative of the porosity of the whole membrane), membrane thickness, tortuosity and pore size distribution. All values were evaluated by statistical image analysis of SEM micrographs using ImageJ software. Details of the measurement method are reported elsewhere (10).

Electroosmotic Experiments

Electroosmotic flow measurements in the CNT membranes were conducted using a custom-made rig and membrane holder described in (6). The membranes were sandwiched between two platinum mesh electrodes (99.99 %, 52 mesh per inch) and placed across two flanges using soft rubber to ensure seal. On each side of the flanges were reservoirs for the electrolyte large enough to avoid any ion depletion. Before the start of the experiments the concentration in the two reservoirs was equimolar to avoid any concentration gradients. First, small pressure gradients were exerted across the membranes (18 – 50 kPa) to record pressure-driven flow across the membrane using pressure transducers (Swagelok industrial standard®, 0.05 bar error). This probed the structural integrity of the membrane and provided a baseline to evaluate EOF. It is noted here that the back pressure experienced in electroosmotic flows in this study was less that 0.01% of the total flow and therefore negligible (2). Pressure-driven flow was imposed using a pressurized liquid reservoir and mass transport through the membrane was recorded (2 second interval) using a balance with 0.1 mg sensitivity. EOF was then superimposed on the pressure-driven flow and the total flow rate measured. Therefore, the EOF is obtained by subtraction of the two. Sodium tetra-borate, $Na_2B_4O_7$ (pH 9.2, 5 mM) and NaCL (2mM) were used as the buffer during the experiments. The applied voltage was $\Delta V_{app} = 10$ V for all experiments. Each measurement lasted 20-40 minutes and was repeated at least three times.

Analysis of Experimental Results

The CNT membranes produced using AAM templates, although having a narrow pore size distribution and tortuosity τ : 1, all have small variations in terms of thickness and effective area. Furthermore, small variations in the applied pressure in the pressure-driven flow case were also observed for each membrane. Therefore, flow rate data has to be normalized to account for these variations to be compared. This is done introducing the concept of permeability (16):

$$K = \frac{Q}{A_m \Delta p} \Rightarrow K_T = K_{EO} + K_{\Delta p} \qquad [12]$$

The permeability K has units $m^3m^{-2}s^{-1}Pa^{-1}$, which is equivalent to the LMH (L m^{-2} h^{-1}@ 1 bar) units more commonly used in the membrane community.

The effective voltage can be obtained from the applied voltage via the following relation:

$$\Delta V_{eff} = \Delta V_{app} - \Delta V_{dec} - 2R_{tot} I \qquad [13]$$

where the first term on the right hand side of the equation represents the externally applied voltage, the second the decomposition potential at the electrodes, equal to ~4.5 V for a platinum electrode/electrolyte solution (11) and the third is the product of the total system resistance and the steady state current (~ 1mA in

the present case). While a direct, *in situ* measurement of R_{tot} is not possible, it is possible to estimate its value at the beginning of the EO experiment, when no concentration polarization has yet developed (6). As can be seen in Figure 1, the current (red solid line) rapidly decreases followed by sudden current shocks, which have been attributed to the propagation of concentration polarization, generating zones of ion enrichment and depletion (17, 18). The resistance follows a specular behaviour, with the resistance value at the start of the experiment being ~ 2000 Ω. Due to experimental uncertainties and measurement errors, a compounded error of 25% is associated with this estimate. It is also noted that this value is significantly higher than what obtained by the authors (6) for alumina membranes (without carbon) under the same experimental conditions (~ 70 Ω). While the CNTs are certainly more conductive than alumina, the CVD process produces a significant increase in the roughness of the membranes' surface (16), which would lead to an increase in resistance of the electrolyte through the membrane. Including all of the above factors in Eq. [13], ΔV_{eff} is estimated to vary between 0.7 and 2.3 V.

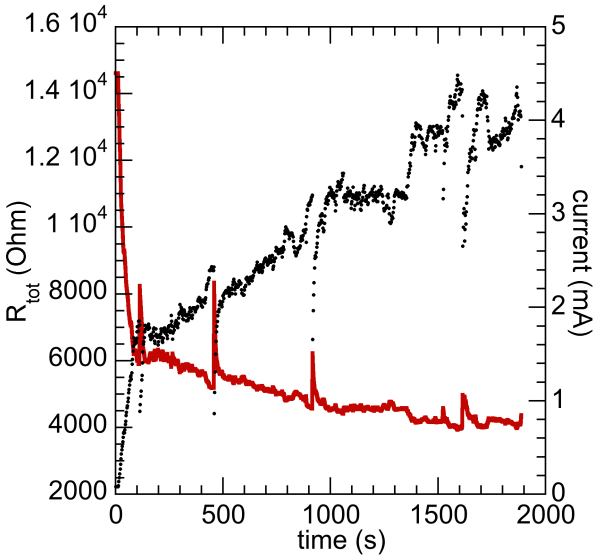

Figure 1. Variation with time of total resistance (filled circle) and current (red solid line) for borate buffer solution, and a membrane with average nanotube diameter of 16 nm. This result is representative for all membranes and conditions tested. Sudden decreases in total resistance are clearly linked to current shocks, which disrupt the concentration polarization layer build-up, which is then resumed until the next current shock. The compounded error of the resistance values is estimated at 25%.

Numerical Analysis

As the experimental conditions in the present work fall close to or within the region of electrical double layer overlap, the simplified solution for $F = 1$ reported in Eq.[11] cannot be applied to the present case and, in fact,

does not accurately reflect experimental data. Therefore, equation [4] has to be used, with a calculated solution for F . This was done considering the full, non-linear P-B Eq. [6] and the linearized one Eq. [7]. The former was solved numerically, while for the latter the exact solution in Eq.[8] was used. Finally, Eq.[5] was integrated numerically. A solution for the numerical resolution of the non-linear P-B equation has been constructed via the following steps:

- Equation [6] has been collocated in equispaced points;
- The differential operators have been discretized via finite differences of order 2;
- Boundary conditions were imposed in strong form;
- The resulting non-linear system was solved using a Modified 2-steps Quasi-Newton algorithm with frozen Jacobian (the exact Jacobian computed in the solution of the linearized problem) and taking as starting point the solution of the linear problem.

The procedure was implemented in Matlab and gives a solution up to machine precision within a few steps of the iterative procedure (< 10) with medium size problems (~ 80 unknowns). The computed solution was then used to calculate an approximation of the integral that defines F : A composite rule of order 2 was used, resulting in a computed value that differs from the exact integral by less than 0.01%.

With the parameters of the P-B equation fixed to one of the experimental settings, the solution of the non-linear problem differs from the solution Eq.[7] of the linearized problem by less than ~ 0.1%, thus this simplification can also be used in the present setting. While for large nanotube diameters, both the non-linear and the linearized P-B have values close to 1, in the region close to EDL overlap, the computed values for F are significantly less than 1, as seen in Figure 2. This provides evidence that using the simplified Eq. [11] for small values of R/λ_D leads to significant errors. The trends are similar (though values differ) for the two electrolytes used

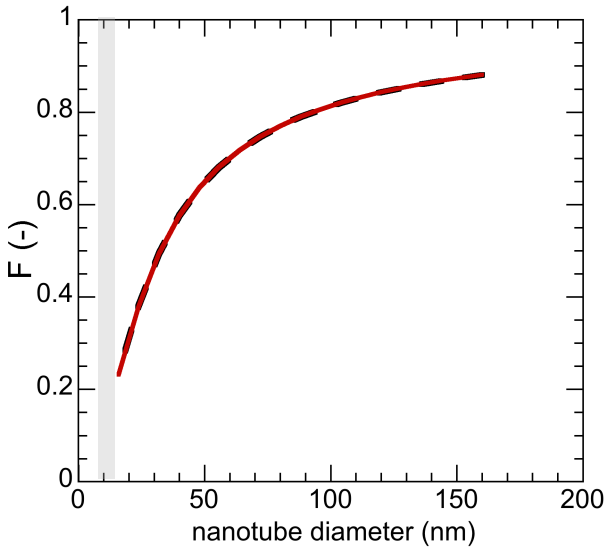

Figure 2. Calculated values for F for the non-linear P-B equation (black dotted curve) and the linearized P-B (red curve) for a borate buffer solution. The band in grey indicates the region of EDL overlap.

Results and Discussion

As the diameter of the CNTs in the membranes decreases, the permeability for the NaCl solution caused by the pressure gradient alone (no applied voltage) across the membrane decreases (Fig. 3-left, black dots), as expected, in agreement with the quadratic dependence on the tube diameter (Fig. 3-left, inset). When the electric field is summed to the pressure one, the total flow is now given by the pressure driven and electroosmotic flows (cfr. Eq. [4]), pumping water in the same direction (Fig. 1-left, white dots). The total permeability is as a result higher and, as the average nanotube diameter approaches the EDL overlap region a remarkable enhancement of the total flow is observed. This is clearer when the ratio of the electroosmotic permeability over the pressure driven one is reported as a function of the CNT diameter (Fig. 3-right). As discussed in the literature, this result is in direct contrast with the simplified treatment of electroosmosis (cfr. Eq.[10]), which assumes no EO flow when the radius of the channel approaches the Debye length.

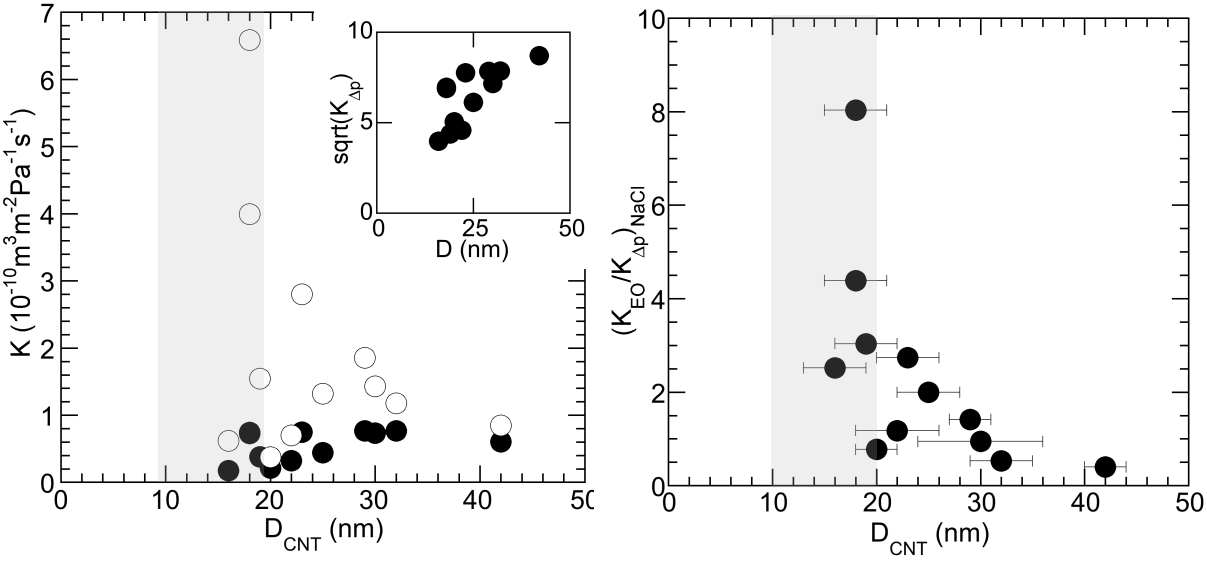

Figure 3. Left: Total permeability ($K_T = K_{\Delta p} + K_{EO}$, empty circles) given by the sum of the pressure-driven (black circles) and EO-driven flows as a function of average CNT diameter. Inset shows the quadratic dependence of the pressure driven flow alone on nanotube diameter. Right: EO flow enhancement ($K_{EO} / K_{\Delta p}$) as a function of average nanotube diameter. Error on permeability values is 5%, whereas standard deviation is reported for CNT diameters only on right plot. The grey band indicates the overlap region, which varies in value as a function of the electrolyte concentration.

In the case of the borate buffer solution, the total permeability data (Fig. 4-left, white dots) is also higher than the pressure driven one (Fig. 4-left, black dots), though the trend is not as pronounced as in the case of the NaCl solution. Nonetheless, when the data is represented as the ratio between the electroosmotic permeability and that from the pressure driven flow (Fig. 4-right), the enhancement is once again very clear. As in the previous case, the square root dependence of the pressure driven permeability on the CNTs diameter is respected (not shown).

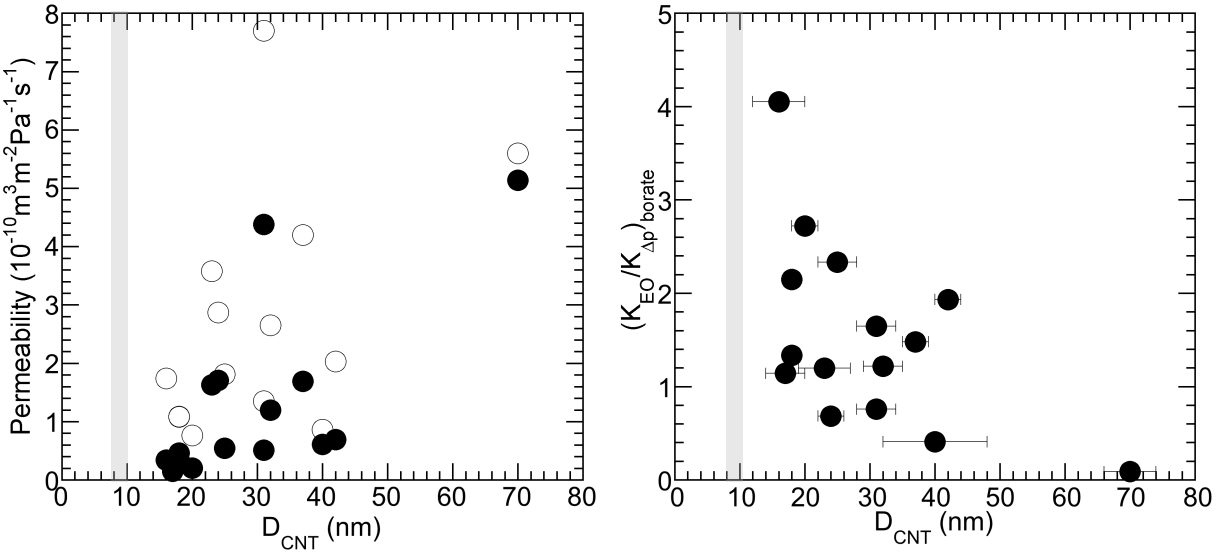

Figure 4. Left: Total permeability ($K_T = K_{\Delta p} + K_{EO}$, empty circles) given by the sum of the pressure-driven (black circles) and EO-driven flows as a function of average CNT diameter. Right: EO flow enhancement ($K_{EO} / K_{\Delta p}$) as a function of average nanotube diameter. Error on permeability values is 5%, whereas standard deviation is reported for CNT diameters only on right plot. The grey band indicates the overlap region.

Results for both electrolyte solutions clearly show not only a significant enhancement of the electroosmotic flow but also net EOF near to or in the region of the electrical double layer overlap, providing direct evidence of the limits of the simplified treatment of EO (i.e. for $F = 1$, Eq.[11]). The latter is commonly (and appropriately) used for EOF in micrometre sized channels, where $R \gg \lambda_D$. At the nanoscale, on the other hand, where the Debye length can be comparable to the channel characteristic dimension, the more complex treatment of EO must be used, either in the form of the non-linear solution or the linearized one for the P-B equation. This result is significant as it means that EOF can be an effective pumping mechanism also at the nanoscale, opening the way for its use in a number of different applications, from membrane-based filtration to further miniaturization of lab-on-a-chip and *in vivo* implants.

If the simplified treatment of EO does not apply at the nanoscale, it remains to be seen whether the linearized P-B equation (Eq. [7]) can be used or the more complex non-linear one is necessary (Eq. [6]). The difference is

not trivial since an exact solution exists for the former while the latter has to be solved numerically. From the analysis in Figure 2, it is clear that for the conditions used in this work, particularly the low zeta potential of the CNTs, justifies using the Debye-Hückel approximation. Therefore the difference between the non-linear and the linear solutions to the P-B equation is negligible. This is confirmed in Figure 5, where the experimental data for the ratio between EO and pressure driven permeabilities for the borate buffer solution is reproduced with the corresponding values for the 2 solutions. As discussed earlier, this might not be the case for other materials more commonly used in EO, such as silica. The ratio between EO and pressure-driven permeabilities is here normalized by the pressure Δp^*, to eliminate this dependence and only show the one from the nanotube diameter.

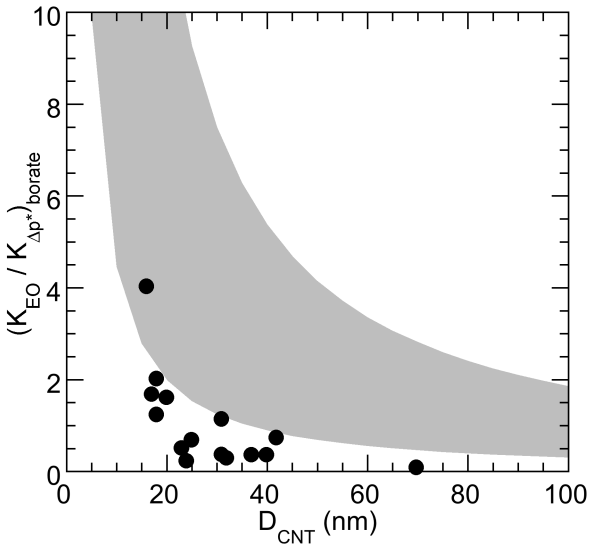

Figure 4. Comparison between experimental data (black dots) and model for linearized solution of P-B (Eq.[8], grey band). The non-linear solution of P-B (Eq. [7]) fully overlaps the one for the linear case. The width of the band represents the compounded error (±25%) associated with the calculation of ΔV_{eff}.

As can be observed, the model overestimates the experimental data in most of the CNT diameter range investigated. This could be attributed either to a larger error in the estimation of the effective voltage, as discussed earlier, or in the measurement of the experimental data (flow rate and or nanotube diameter). Another possibility can be the fact that the no-slip boundary condition has been used to solve the Navier-Stokes equation with the electroosmotic term. There is ample evidence in the literature, including for the same nanotubes used in this work, that a significant amount of wall slip is present for water flowing through carbon nanotubes under a pressure gradient. Considering slip could alter the permeability values resulting from applying the model to the present case, at least in the pressure-driven flow case, though whether slip is

possible in the case of an electrolyte solution near a charged surface is a yet unsolved problem (1), beyond the scope of this work.

Conclusions

In summary, experimental evidence of the presence of electroosmotic flow in carbon nanotube membranes close or in the region of electrical double layer overlap is presented for two different electrolytes for the first time. These results show that predictions that no EOF would be observed in the region of EDL overlap are incorrect, as they are based on simplifying assumptions valid only at the microscale but not at the nanoscale. As such, a more complex theoretical framework has to be used, based on the Poisson-Boltzmann equation describing the electrical potential in the electrolyte and near the charged surface. A numerical analysis of both the solutions for the non-linear and the linearized P-B equations show that for the specific material used in this work, carbon nanotubes, the simpler, linearized solution can be adopted with little error. The experimental data and the theoretical analysis are important as they open the way to using electroosmotic pumping in a wide range of applications, from membrane-based filtration (as a more efficient alternative to mechanical pumping in the ultrafiltration and nanofiltration range) to further miniaturization of lab-on-a-chip devices for *in vivo* implantation.

Additional Information

Data Accessibility
All data supporting this study are provided as supplementary information accompanying this paper.

Authors' Contributions
HL carried out the experiments. FC performed the numerical simulations; DM performed data analysis, conceived of and designed the study, and drafted the manuscript. All authors read and approved the manuscript.

Competing Interests
The authors declare that they have no competing interests".

Funding Statement
DM and HL to acknowledge the UK EPSRC (grant number EP/G045798/1) for funding; DM also acknowledges the Royal Academy of Engineering for funding.

References

1. Chang H-C, Yeo LY. Electrokinetically Driven Microfluidics and Nanofluidics: Cambridge University Press; 2010.
2. Bruus H. Theoretical Microfluidics: Oxford University Press; 2008.
3. Rice CL, Whitehead R. Electrokinetic Flow in a Narrow Cylindrical Capillary. The Journal of Physical Chemistry. 1965;69(11):4017-24.
4. Wu J, Gerstandt K, Majumder M, Zhan X, Hinds BJ. Highly efficient electroosmotic flow through functionalized carbon nanotube membranes. Nanoscale. 2011;3(8):3321-8.
5. Kemery PJ, Steehler JK, Bohn PW. Electric Field Mediated Transport in Nanometer Diameter Channels. Langmuir. 1998;14(10):2884-9.
6. Leese H, Mattia D. Electroosmotic flow in nanoporous membranes in the region of electric double layer overlap. Microfluid Nanofluid. 2014;16(4):711-9.
7. Freund JB. Electro-osmosis in a nanometer-scale channel studied by atomistic simulation. The Journal of Chemical Physics. 2002;116(5):2194-200.
8. Chen Y, Ni Z, Wang G, Xu D, Li DY. Electroosmotic Flow in Nanotubes with High Surface Charge Densities. Nano Lett. 2008;8(1):42-8.
9. Cazade P-A, Hartkamp R, Coasne B. Structure and Dynamics of an Electrolyte Confined in Charged Nanopores. The Journal of Physical Chemistry C. 2014;118(10):5061-72.
10. Lee KP, Leese H, Mattia D. Water flow enhancement in hydrophilic nanochannels. Nanoscale. 2012;4(8):2621-7.
11. Yao S, Hertzog DE, Zeng S, Mikkelsen Jr JC, Santiago JG. Porous glass electroosmotic pumps: design and experiments. J Colloid Interface Sci. 2003;268(1):143-53.
12. Bowen WR, Jenner F. Electroviscous Effects in Charged Capillaries. J Colloid Interface Sci. 1995;173(2):388-95.
13. Yao S, Santiago JG. Porous glass electroosmotic pumps: theory. J Colloid Interface Sci. 2003;268(1):133-42.
14. Miller SA, Young VY, Martin CR. Electroosmotic Flow in Template-Prepared Carbon Nanotube Membranes. J Am Chem Soc. 2001;123(49):12335-42.
15. Mattia D, Rossi MP, Kim BM, Korneva G, Bau HH, Gogotsi Y. Effect of Graphitization on the Wettability and Electrical Conductivity of CVD Carbon Nanotubes and Films. J Phys Chem B. 2006;110(20):9850 -5.
16. Mattia D, Leese H, Lee KP. Carbon nanotube membranes: From flow enhancement to permeability. J Membr Sci. 2015;475(0):266-72.
17. Suss ME, Mani A, Zangle TA, Santiago JG. Electroosmotic pump performance is affected by concentration polarizations of both electrodes and pump. Sensors and Actuators A: Physical. 2011;165(2):310-5.
18. Mani A, Zangle TA, Santiago JG. On the Propagation of Concentration Polarization from Microchannel−Nanochannel Interfaces Part I: Analytical Model and Characteristic Analysis. Langmuir. 2009;25(6):3898-908.